Dynamic modelling of the heat transfer into the cooling screen of the SFGT-Gasifier

Julia Kittel[1] Frank Hannemann[2] Friedemann Mehlhose[2] Sindy Heil[1] Bernd Meyer[1]

[1]Institut of Energy Process Engineering and Chemical Engineering
TU Bergakademie Freiberg
09596 Freiberg

[2]Siemens Fuel Gasification Technologie GmbH & Co.KG
Halsbrückerstraße 34
09599 Freiberg

Julia.Kittel@iec.tu-freiberg.de

Abstract

The paper deals with the transient modelling of the heat flux into the cooling screen of the SFGT-Gasifier. Therefore the modelling assumptions and the implementation in Modelica/Dymola were described.

Keywords: SFGT-Gasifier, heat transfer, slag layer modelling, cooling screen

1 Introduction

The SFGT-Gasifier is an entrained flow gasifier. Coal consisting of fixed carbon, volatiles, ash and water is converted at high pressure (about 40 bars) and high temperature (1400-1700 °C) conditions and by addition of oxygen into a synthesis gas (syngas) composed primarily of carbon monoxide (CO) and hydrogen (H_2).

An advantage of the SFGT-Gasifier is the utilization of a cooling screen instead of refractory lining allowing a fast start-up-process. The cooling screen is composed of a castables layer and a helical tube with water as cooling medium (Figure 1).

An entrained flow gasifier is operated at high temperatures well above the ash melting temperature (T > 1300 °C). The molten ash (called slag) accumulates on the internal walls of the reaction chamber due to drag forces. And hence, a liquid slag layer is formed. Between molten slag and cold castables a layer of solidified slag appears. The thickness of the slag layer depends on the process conditions.

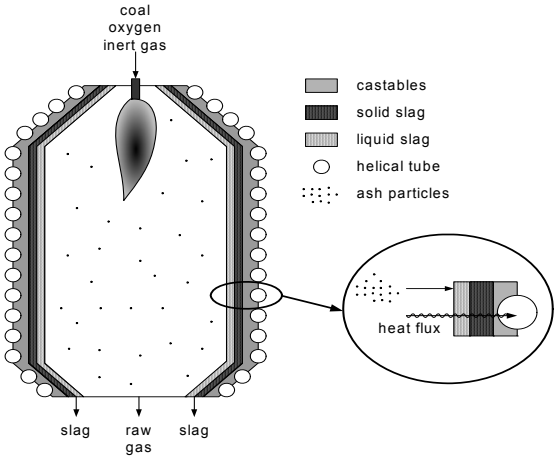

Figure 1: Schematic illustration of the reaction chamber of the SFGT-Gasifier and slag deposit

Hence any dynamical change of heat flux indicates variation in gasifier performance and can be used for better operational control. For this reason it is of great interest to simulate the slag layer formation since the slag layer is the limiting factor for the heat flux, due to the small thermal conductivity of the slag.

DOI: 10.3384/ecp09430011

2 Gasification fundamentals

2.1 Gasification in general

The gasification process is of great importance for the power and basic chemical industry as it coverts any carbon-containing material into a syngas composed primarily of carbon monoxide and hydrogen. This syngas can be used as a fuel in a combined cycle to generate electricity (Integrated Gasification Combined Cycle). But it can also be used as a feedstock for a large number of syntheses in the chemical industry, gaining products like methanol, methane, ammonia or hydrocarbons (Fischer Tropsch Synthesis).

Gasification means the thermo-chemical conversion of fuels with one or more reactants to a combustible gas, which is desirably rich of components CO, H_2 and methane (CH_4). The most proceeded reactions are the partial oxidations, which take place with oxygen in free (molecular) or bounded form (steam (H_2O), carbon monoxide (CO_2)). These partial oxidations are interfered in dependence on the process and the process parameters with pyrolysis or devolatilization and hydrogenation processes [1].

The gasification process can be classified into different types according to the heat supply (autothermic, allothermic or hydrogenating gasification), the gas-solid-contacting (fixed/moving bed, fluidized bed or entrained flow gasification) or concerning the process temperature (above or below the ash melting point).

In the gasification process a large number of reactions take place. Principle chemical reactions are those involving carbon (C), carbon monoxide, carbon dioxide, hydrogen, water (or steam) and methane [2]:

Combustion reactions:

$$C + 0.5\ O_2 \rightarrow CO \qquad -111\ \text{MJ/kmol}$$
$$CO + 0.5\ O_2 \rightarrow CO_2 \qquad -283\ \text{MJ/kmol},$$
$$H_2 + 0.5\ O_2 \rightarrow H_2O \qquad -242\ \text{MJ/kmol}$$

Boudouard reaction:

$$C + CO_2 \leftrightarrow 2\ CO \qquad +172\ \text{MJ/kmol},$$

Water gas reaction:

$$C + H_2O \leftrightarrow CO + H_2 \qquad +131\ \text{MJ/kmol},$$

Hydrogenation reaction:

$$C + 2\ H_2 \leftrightarrow CH_4 \qquad -75\ \text{MJ/kmol},$$

CO Shift reaction:

$$CO + H_2O \leftrightarrow CO_2 + H_2 \qquad -41\ \text{MJ/kmol},$$

Steam reforming reaction

$$CH_4 + H_2O \leftrightarrow CO + 3\ H_2 \qquad +206\ \text{MJ/kmol}.$$

Most fuels contain additional components beside carbon, hydrogen and oxygen, e.g. sulfur, nitrogen or minerals. Sulphur in the fuel is converted into H_2S and COS and the nitrogen into molecular nitrogen, NH_3 or HCN.

2.2 SFGT-Gasifier

The SFGT-Gasifier is a top fired, dry feed, autothermic, oxygen blown, entrained flow gasifier with temperatures in the gasification section well above the ash melting point. The slag and the hot gasification gas leave the gasification section together. After gasification section the hot gas is cooled down in the quench by injection of cold water.

Figure 2 shows the schematic design of the SFGT-Gasifier.

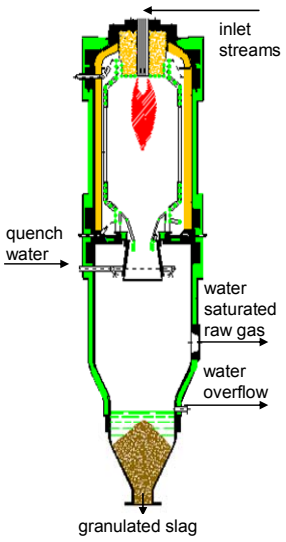

Figure 2: Schematic design of the SFGT-Gasifier

3 Theoretical background

3.1 Equilibrium calculation for the gasification process

For an entrained flow gasifier it can be assumed that the raw gas leaving the reaction chamber is in chemical equilibrium due to high temperatures.

There are two general alternatives to calculate a chemical equilibrium: equilibrium due to reaction equilibria or equilibrium due to minimization of the Gibbs free energy.

Here the minimization of the Gibbs free energy was adopted:

$$G\left(\{n_j\}\right)=\sum_{j=1}^{N_S}\mu_j\cdot n_j=\min!,\quad T,p=const \tag{1}$$

where G is the Gibbs free energy, μ_j is the chemical potential of chemical substance j, n_j is the mol quantity of chemical substance j and N_S is the number of chemical substances.

Under the side conditions:

$$\sum_{j=1}^{N_S}a_{ij}\cdot n_j=b_i,\quad i=1,...,N_E \tag{2}$$

where b_i is the quantity of chemical element i, $\{a_{ij}\}$ is the elemental matrix and N_E is the number of chemical elements.

For the modelling of the heat flux through the cooling screen of the SFGT-Gasifier only the typical chemical gasification substances CO, CO_2, CH_4, H_2, H_2O, H_2S, N_2, O_2 and fixed carbon have to be considered for the calculation of the chemical equilibrium.

The constrained optimization problem can be solved through conversion in an unconstrained minimization problem by adoption of Lagrange multipliers $\{\lambda_i\}$ [3]:

$$L\left(\{n_j\},\{\lambda_k\}\right)=\sum_{j=1}^{N_S}\mu_j\cdot n_j+\sum_{i=1}^{N_E}\lambda_i\left(b_i-\sum_{j=1}^{N_S}a_{ij}\cdot n_j\right)=\min! \tag{3}$$

This can be transferred in a set of (N_S+N_E) nonlinear equations:

$$\begin{aligned}\frac{\partial L}{\partial n_j}&=0=\mu_j+\sum_{i=i}^{N_E}a_{ij}\cdot\lambda_i & j&=1,...,N_S\\ \frac{\partial L}{\partial \lambda_i}&=0=b_i-\sum_{j=1}^{N_S}a_{ij}\cdot n_j & i&=1,...,N_E\end{aligned} \tag{4}$$

Nonlinear equation system (4) can be solved e.g. by application of the Newton algorithm.

The above introduced equations are only valid for constant temperature and pressure. But the equilibrium temperature of the gasification gas is unknown. Therefore the output temperature of the gasification gas is iteratively calculated by solving the energy balance equation:

$$\sum_k\dot{H}_{in,k}+H_{u,k}\cdot\dot{m}_{k,in}=\sum_j\dot{H}_{out,j}+H_{u,j}\cdot\dot{m}_{j,out}+\Delta h_m\cdot\dot{m}_{ash,in} \tag{5}$$

where k belongs to coal, gasification agent and additional input gases; j belongs to gasification gas, ash/slag and remaining fixed carbon. Furthermore H_u represents the lower heating value, $\dot{H}_{in}$ the entering enthalpy flow, and $\dot{H}_{out}$ the outgoing enthalpy flow. Δh_m is the melting enthalpy of the coal ash and $\dot{m}_{ash,in}$ the incoming coal ash mass flow rate.

3.2 Heat transfer

The heat transfer from the hot, particle loaded gasification gas to the slag layer is due to radiation and convection, whereupon the convective heat transfer can be neglected [4].

For calculation of radiative heat transfer the coupled gas and particle radiation has to be considered. Thereby CO, CO_2, CH_4 and H_2O are radiation absorbing gas components. Due to the fact that there is only less material about the calculation of the emission coefficients for CO under high pressure, CO is handled as CO_2 in the equations as *Fleischer* has done [5].

For the hot gasification process the radiation due to increased particle loading has to be regarded. Then the heat flux $\dot{Q}_{rad}$ owing to the coupled gas-particle radiation can be defined as [6]:

$$\dot{Q}_{rad}=A\cdot\sigma\cdot\beta\cdot\left(\varepsilon_{G+P}\cdot T_G^4-\alpha_{G+P}\cdot T_{G\to S}^4\right)$$
$$\beta=\frac{\varepsilon_S}{\alpha_{G+P}+\varepsilon_S-\alpha_{G+P}\cdot\varepsilon_S}, \tag{6}$$

where A is the heat transfer area, σ is the Boltzmann constant, T_G is the gas temperature, $T_{G\to S}$ is the surface temperature of the liquid slag layer, ε_S is the emission coefficient of the slag, ε_{G+P} and α_{G+P} are the emission and the absorption coefficient of the particle loaded gas, respectively. Modeling equations and parametric tables for ε_{G+P} and α_{G+P} can be found in *VDI Wärmeatlas* [6].

For the emission coefficient of slag the fixed value of $\varepsilon_S=0.83$ is assumed [7].

3.3 Helical tube

For calculation the heat flow due to water side convection the fluid flow conditions have to be known. With the Nusselt number Nu the heat transfer coefficient α can be calculated:

$$\mathrm{Nu}=\frac{\alpha}{\lambda}\cdot d_0 \tag{7}$$

where d_0 is the internal diameter of the pipe and λ is the thermal conductivity of the fluid.

Literature provides different equations for calculation of Nusselt numbers in helical tubes. An overview about some of them can be found in *Kumar et al* [8].

The following explanations refer to *VDI Wärmeatlas* [6].

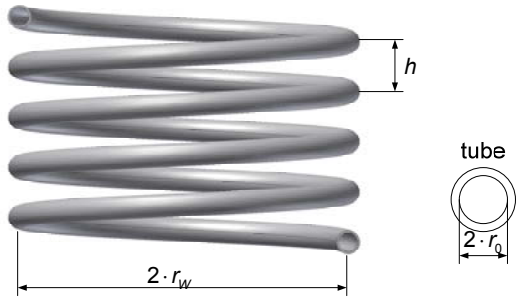

Figure 3: Helical tube

Figure 3 shows schematically a helical tube. The critical Reynolds number Re_{crit} to define the flow condition is defined as:

$$\mathrm{Re}_{crit} = 2300 \cdot \left[1 + 8.6 \cdot \left(\frac{d_0}{D} \right)^{0.45} \right] \tag{8}$$

D is the middle curve diameter of the helical tube.

For laminar flow conditions $\left(\mathrm{Re} \le \mathrm{Re}_{crit}\right)$ the Nusselt number is calculated as:

$$\mathrm{Nu}_l = \beta \cdot \left(\frac{\mathrm{Pr}}{\mathrm{Pr}_W} \right)^{0.14}$$

where:

$$\beta = \left(3.66 + 0.08 \cdot \left[1 + 0.8 \cdot \left(\frac{d_0}{D} \right)^{0.9} \right] \cdot \mathrm{Re}^m \cdot \mathrm{Pr}^{1/3} \right) \tag{9}$$

$$m = 0.5 + 0.2903 \cdot \left(\frac{d_0}{D} \right)^{0.194}$$

For turbulent flow conditions $\left(\mathrm{Re} \ge 2.2 \cdot 10^4\right)$ the Nusselt Number is defined as:

$$\mathrm{Nu}_t = \frac{0.125 \cdot \xi \cdot \mathrm{Re} \cdot \mathrm{Pr}}{1 + 12.7 \cdot \sqrt{0.125 \cdot \xi} \cdot \left(\mathrm{Pr}^{2/3} - 1 \right)} \cdot \left(\frac{\mathrm{Pr}}{\mathrm{Pr}_W} \right)^{0.14} \tag{10}$$

$$\xi = \frac{0.3164}{\mathrm{Re}^{0.25}} + 0.03 \cdot \left(\frac{d}{D} \right)^{0.5}$$

And for the transition zone $\left(\mathrm{Re}_{crit} < \mathrm{Re} < 2.2 \cdot 10^4\right)$:

$$\mathrm{Nu} = \eta \cdot \mathrm{Nu}_l\left(\mathrm{Re}_{crit}\right) + \left(1 - \eta\right) \mathrm{Nu}_t\left(\mathrm{Re} = 2.2 \cdot 10^4\right) \tag{11}$$

$$\eta = \frac{2.2 \cdot 10^4 - \mathrm{Re}}{2.2 \cdot 10^4 - \mathrm{Re}_{crit}}$$

3.4 Slag properties

Coal slag is a multi-phase system. The main components are SiO_2, CaO, MgO, Fe_2O_3 and Al_2O_3.

To implement a slag building model the physical properties of the slag such as thermal conductivity or viscosity must be known. Most of the physical properties are dependent on temperature and composition of the coal ash.

3.4.1 Slag Viscosity

There are a lot of empirical viscosity models obtainable from literature. A summary of these models can be found in *Vargas et al* [9]. At this point only the *Kalmanovitch-Frank Model* shall be shortly introduced, because this model reflects the viscosity of coal slags with sufficient accuracy [9][10].

The *Kalmanovitch-Frank Model* is based on the Weymann-Correlation:

$$\log \eta = \log a + \log T + b / T \tag{12}$$

For calculation of the parameters a and b slag components were classified into glass builder (x_g), glass modifier (x_m) and amphoterics (x_a):

$$x_g = \zeta_{\mathrm{SiO_2}} + \zeta_{\mathrm{P_2O_5}}$$

$$x_m = \zeta_{\mathrm{FeO}} + \zeta_{\mathrm{CaO}} + \zeta_{\mathrm{MgO}} + \zeta_{\mathrm{Na_2O}} + \zeta_{\mathrm{K_2O}} + \zeta_{\mathrm{MnO}} + \zeta_{\mathrm{NiO}} + 2\left(\zeta_{\mathrm{TiO_2}} + \zeta_{\mathrm{ZrO_2}}\right) + 3\zeta_{\mathrm{CaF_2}}$$

$$x_a = \zeta_{\mathrm{Al_2O_3}} + \zeta_{\mathrm{Fe_2O_3}} + \zeta_{\mathrm{B_2O_3}}$$

where ζ_i is the mass fraction of component i.

With these mass fractions the parameters a and b can be computed as:

$$b = 10^3 \cdot \left(b_0 + b_1 \cdot \zeta_{\mathrm{SiO_2}} + b_2 \cdot \zeta_{\mathrm{SiO_2}}^2 + b_3 \cdot \zeta_{\mathrm{SiO_2}}^3 \right)$$

$$a = \exp\left(-0{,}2812 \cdot 10^{-3} \cdot b - 14{,}1305\right)$$

With:

$$b_0 = 13.8 + 39.9355 \cdot \alpha - 44.049 \cdot \alpha^2$$

$$b_1 = 30.481 - 117.1505 \cdot \alpha + 129.9978 \cdot \alpha^2$$

$$b_2 = -40.9429 + 234.0486 \cdot \alpha - 300.04 \cdot \alpha^2$$

$$b_3 = 60.7619 - 153.9276 \cdot \alpha + 211.1616 \cdot \alpha^2$$

$$\alpha = \frac{x_m}{x_m + x_a}$$

3.4.2 Thermal conductivity

The thermal conductivity of slag is one of the physical properties with the largest influence on the heat flow rate through the slag layer [11]. Literature shows only some mathematical models available for the calculation of the thermal conductivity.

Here the following mathematical model which was also used by *Seggiani* [12] was implemented:

$$\lambda_S = \alpha \cdot c_p \cdot \rho$$

with:

$$\alpha = 4.5 \cdot 10^{-7}\ \mathrm{m^2/s} \qquad (13)$$
$$c_p = 1100\ \mathrm{J/(m\,K)}$$
$$\rho = 2500\ \mathrm{kg/m^3}$$

4 Implementation of the Model in Modelica/Dymola

4.1 Model development

As base for the modelling of heat flux through the cooling-screen of the SFGT-Gasifier the Modelica Fluid 1.0 Library connectors were used. The components for modelling a gasifier do not exist in a Modelica library. This extension was developed.

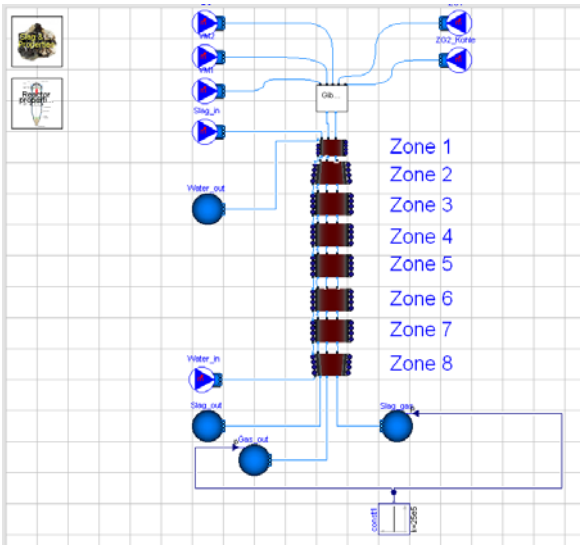

Figure 4: Implementation of the SFGT-Gasifier model in Modelica/Dymola

The gasification section including the cooling screen was modelled by division into several zones (Figure 4). In the first zone the thermo-chemical equilibrium is calculated by minimization of Gibbs free energy. Therefore, a Dynamic Link Library (DLL) was implemented in C and was inserted into the Modelica model as an external function.

In the following zones slag layer thickness and heat transfer from the hot raw gas to the cooling water (heat flux zones) are calculated. The number of heat flux zones depends on the size of the gasifier.

Furthermore, two system components have to be included in the simulation model. The system component "slag" comprises the composition of slag and coal in order to calculate the slag properties. The "slag" component provides also the opportunity to include experimentally determined correlations for slag properties.

In the component "reactor" the dimensions of the gasifier like diameters of pipes and the properties of wall materials are configured.

Each heat flux zone is built up of 3 sections (Figure 5): the gas compartment, the solid materials (liquid and solid slag layer, castables layer and helical tube material) and the cooling water. Between these sections occur heat and mass transfer as shown in Figure 6. For each section the energy and mass conservation equations are solved, the momentum conservation equations are neglected.

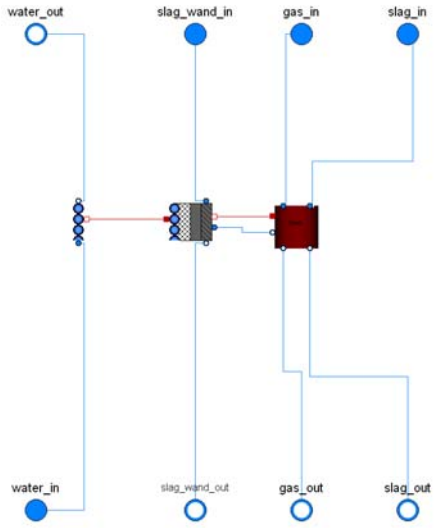

Figure 5: Implementation of one heat flux zone in Modelica/Dymola

It has to be noted that the composition of the gas leaving the last heat flux zone does not belong exactly to the equilibrium composition at the outlet temperature. But the differences in the equilibrium composition for the equilibrium state with and without heat loss, respectively, are only small due to the high temperatures.

4.2 Gas compartment

The gas compartment is assumed as a continuously stirred-tank reactor. The following mass balances are regarded:

$$\frac{\mathrm{d}\,m_{G,i}}{\mathrm{d}\,t} = \dot{m}_{G,in,i} + \dot{m}_{G,out,i} \qquad (14)$$

$$\frac{\mathrm{d}\,m_{S,i}}{\mathrm{d}\,t} = \dot{m}_{S,in,i} + \dot{m}_{S,out,i} + \dot{m}_{S,wall,i} = 0 \qquad (15)$$

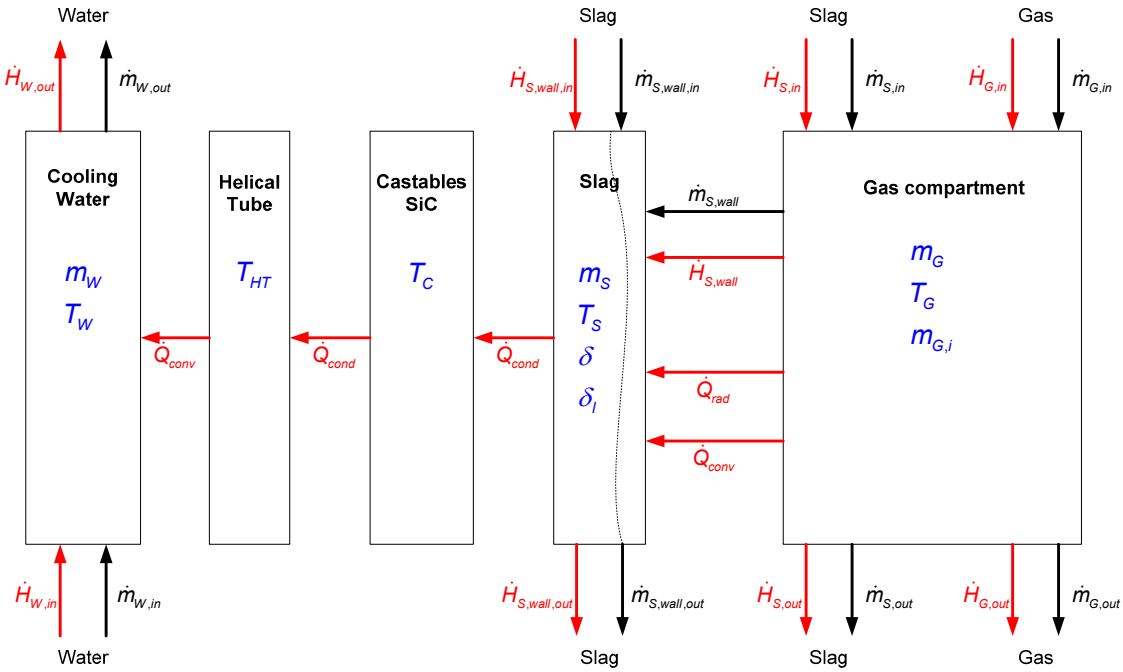

Figure 6: Heat and mass flow for one heat flux zone

where $m_{G,i}$ is the mass of gasification gas, $m_{S,i}$ is the mass of slag, $\dot{m}_{G,in,i}$ and $\dot{m}_{G,out,i}$ are the incoming and leaving gas mass flow rate and $\dot{m}_{S,in,i}$ and $\dot{m}_{S,out,i}$ are the incoming and leaving slag mass flow rate.

Equation (15) means no slag storage in the gas compartment. The fraction of incoming slag mass flow rate accumulating at liquid slag layer $\dot{m}_{S,wall,i}$ can be specified by the user.

For the energy balance of the gas compartment in addition to the in- and out-flowing streams the gas radiation heat flow $\dot{Q}_{G\to S,i}$ has to be considered:

$$\frac{\mathrm{d}U_{G,i}}{\mathrm{d}t} = \dot{H}_{S,in,i} + \dot{H}_{S,out,i} + \dot{H}_{S,wall,i} + \dot{H}_{G,in,i} + \dot{H}_{G,out,i} + \dot{Q}_{G\to S,i} \tag{16}$$

For the calculation of specific enthalpy for the slag mass flow rate accumulating at liquid slag layer the gas temperature is assumed.

4.3 Solid materials

4.3.1 Slag Layer

For the implementation of the slag layer modelling, assumptions of the slag building model by *Reid and Cohen* [12] were used:

(1) The transition temperature between the solid and the liquid slag layer is the temperature of critical viscosity.

(2) The flow of liquid slag is of Newtonian type and the flow at temperatures below T_{CV} is negligible.

(3) The shear stress between gas and slag layer is negligible.

(4) The temperature profile across the slag layer is linear.

(5) The heat transfer occurs perpendicularly to the surface.

(6) The model is written in linear coordinates, owning to a large difference between slag deposit thickness and gasifier radius.

(7) The density, specific heat and thermal conductivity of slag are independent on temperature.

Mass balance for the slag:

$$\frac{\mathrm{d}m_{S,i}}{\mathrm{d}t} = \dot{m}_{S,in,i} + \dot{m}_{S,out,i} + \dot{m}_{S,wall,i} \tag{17}$$

where $m_{S,i}$ is the slag mass, $\dot{m}_{S,in,i}$ is the incoming slag mass flow rate, $\dot{m}_{S,out,i}$ is the discharging slag mass flow rate and $\dot{m}_{S,wall,i}$ is the mass flow rate impacting on the liquid slag layer.

The discharging mass flow rate is calculated due to the assumption that the slag can be considered as a Newtonian fluid. Then the weight F_w equals the friction force F_f in steady state:

$$F_f = F_w$$

Hence:

$$F_f = \eta \cdot A \cdot \frac{\mathrm{d}u_y}{\mathrm{d}x} = b \cdot h \cdot \eta \cdot \frac{\mathrm{d}u_y}{\mathrm{d}x} \qquad (18)$$

$$F_w = m \cdot g = (\delta_l - x) \cdot b \cdot h \cdot \rho \cdot g$$

where η is the viscosity, A is the area, b is the length of the slag layer, h is the height of the slag layer, u_y is the velocity in vertical direction, δ_l is the thickness of the liquid slag layer, m the mass of the slag, ρ the density of the slag and x the horizontal position.

Hence, the change in velocity at each horizontal location x can be defined as:

$$\frac{\mathrm{d}u_y}{\mathrm{d}x} = \frac{(\delta_l - x) \cdot \rho \cdot g}{\eta(T(x))}.$$

By integration of this equation under the boundary condition that the velocity at the boundary layer between liquid and solid slag layer equals zero the equation for velocity results to:

$$u_y(x) = \frac{\rho_S \cdot g}{\eta(T(x))} \cdot \left(\delta_{l,i} \cdot x - \frac{x^2}{2} \right). \qquad (19)$$

So the discharging slag mass flow rate can be calculated as:

$$\dot{m}_{S,out,i} = \rho_S \cdot b_i \cdot \int_{x=0}^{\delta_{l,i}} u_y(x)\,\mathrm{d}x. \qquad (20)$$

The thickness of the liquid slag layer is estimated under the assumption of linear temperature distribution as:

$$\delta_{l,i} = 0.5 \cdot \frac{T_{G\to S,i} - T_{crit}}{T_{G\to S,i} - T_{S,i}} \cdot \delta_i. \qquad (21)$$

Where $T_{G\to S,i}$ is the surface temperature of the liquid slag layer, $T_{S,i}$ is the middle slag layer temperature, T_{crit} is the temperature of critical viscosity and δ_i is the thickness of the slag layer.

Energy conservation equation for the slag

$$\frac{\mathrm{d}U_{S,i}}{\mathrm{d}t} = \dot{H}_{S,in,i} + \dot{H}_{S,out,i} + \dot{H}_{S,wall,i} + \dot{Q}_{G\to S} + \dot{Q}_{S\to C}$$

where for the temperature of discharging slag $T_{S,out,i}$ the middle temperature of the liquid slag layer is assumed. The heat flux from the slag layer to the castables layer is defined as:

$$\dot{Q}_{S\to C} = \frac{T_{S,i} - T_{C,i}}{R_{\lambda,i}}$$

$$\text{with:} \quad R_{\lambda,i} = \frac{1}{A_i} \cdot \left(\frac{0.5 \cdot \delta_i}{\lambda_S} + \frac{0.5 \cdot \delta_C}{\lambda_C} \right), \qquad (22)$$

where $T_{C,i}$ is the middle temperatures of the castables layer, δ_C is the thickness of the castables layer and λ_C is the thermal conductivity of the castables layer.

4.3.2 Castables layer and helical tube material

For the castables layer and the helical tube material only the energy conservation equations have to be considered:

$$\frac{\mathrm{d}E_C}{\mathrm{d}t} = \dot{Q}_{S\to C} + \dot{Q}_{C\to HT}$$

$$\frac{\mathrm{d}E_{HT}}{\mathrm{d}t} = \dot{Q}_{C\to HT} + \dot{Q}_{HT\to W} \qquad (23)$$

The heat flux from the castables layer to the helical tube material is defined as (linear temperature distribution):

$$\dot{Q}_{C\to HT} = \frac{T_{C,i} - T_{HT,i}}{R_{\lambda,i}}$$

$$\text{with:} \quad R_{\lambda,i} = \frac{1}{A_i} \cdot \left(\frac{0.5 \cdot \delta_{HT}}{\lambda_{HT}} + \frac{0.5 \cdot \delta_C}{\lambda_C} \right), \qquad (24)$$

where $T_{HT,i}$ are the middle temperatures of helical tube material, δ_{HT} is the thickness of helical tube material and λ_{HT} is the thermal conductivity of helical tube.

4.4 Cooling water

The cooling water in the helical tube in each heat transfer zone is implemented as a water volume with a heat port. The characteristic flow numbers are calculated due to the actual flow conditions. Then the heat transfer coefficient α_i for the convective heat transfer rate is calculated in a separate function. The following heat and mass balance equations were implemented for each water volume:

$$\frac{\mathrm{d}m_{W,i}}{\mathrm{d}t} = \dot{m}_{W,in,i} + \dot{m}_{W,out,i}$$

$$\frac{\mathrm{d}U_{W,i}}{\mathrm{d}t} = \dot{H}_{W,in,i} + \dot{H}_{W,out,i} + \dot{Q}_{HT\to W} \qquad (25)$$

where the heat flow rate from the helical tube to the cooling water is calculated as:

$$\dot{Q}_{HT\to W} = \alpha_i \cdot A_i \cdot (T_{HT\to W} - T_W) \qquad (26)$$

where $T_{HT \rightarrow W}$ is the surface temperature of the helical tube material and T_W is the temperature of the cooling water.

5 Simulation results

The Modelica/Dymola model could be steady state and transient validated with data of the Siemens test facility located in Freiberg.

Therefore, the input streams (e.g. coal mass flow rate, temperatures, gasification agent mass flow rate…) of the test facility were loaded to the model as a Modelica TimeTable.

As shown in Figure 7 the model provides good correlation with the test data for different evaluation points and various kinds of coal. By means of Figure 7 it can also be shown that the *Kalmanovitch-Frank Model* for calculation of the slag viscosity provides sufficient agreement for calculation of heat flux compared to experimentally determined viscosity.

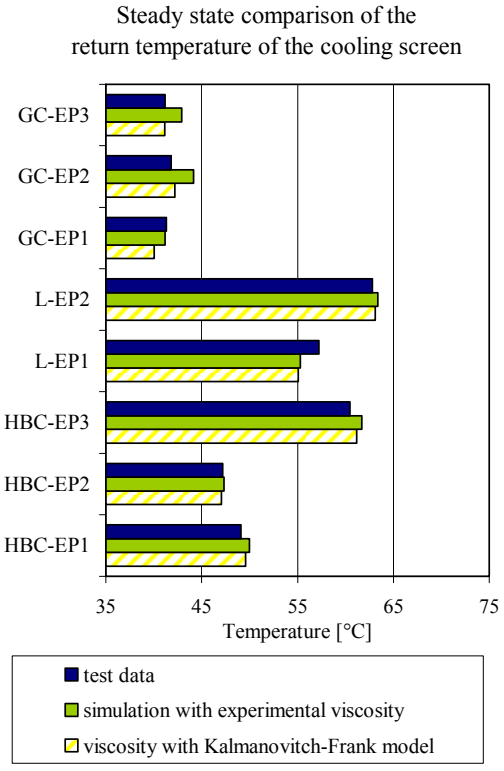

Figure 7: Steady state validation of the model with test data of the Siemens test facility located in Freiberg (In the figure GC means Gas Coal, L belongs to Lignite and HBC to Hard Brown Coal.)

Figure 8 shows the developing of the return temperature of the cooling screen cycle water for a break down of the coal mass flow at time 197 min.

For the regular operation the difference between the simulated and the measured temperature are mostly less than 2 K. As the coal mass flow breaks down and the gasifier operates only with gaseous fuel the difference increases up to 5 K. The cause of this is the calculation of the absorption coefficients for the gas components due to the fact that for the above case the slag layer surface temperature is above the area of validity for these equations. So the value for the absorption coefficient is oversized compared to the emission coefficient. Hence, the heat flow rate from the gas to the slag layer is underestimated.

6 Conclusions

In the article the modelling of the heat flux through the slag coated cooling screen of the SFGT-Gasifier was shown. It could be demonstrated that the developed model reflects the test facility data both steady state and transient with sufficient precision.

The next step will be the scale up of the model to the industrial plant.

References

[1] Klose, E.; Toufar, W.: Grundlagen der Vergasung, 1. Lehrbrief. Lehrbriefe für das Hochschulfernstudiun, 1985

[2] Higman, C.; van der Burgt, M.: Gasification. Gulf Professional Publishing, Amsterdam, 2002

[3] Smith, W.R.; Missen, R.W.: Chemical Reaction Equilibrium Analysis: Theory and Algorithms. John Wiley and Sons, 1982

[4] Brummel, H.-G.; Kakara, E.: Wärmestrahlungsverhalten von Gas-/Feststoffgemischen bei niedrigen, mittleren und hohen Staubbeladungen. In: Wärme- und Stoffübertragung 25 (1990), 129-140

[5] Fleischer, Thomas: Erarbeitung eines Modells zur Berechnung der Wärmeübertragung auf die Kühlschirmwand unter Berücksichtigung der Schlackeeigenschaften. Freiberg, Bergakademie, Fachbereich Maschinen-, Verfahrens- und Energietechnik. Diploma thesis, 2007

[6] Verein Deutscher Ingenieure, VDI-Gesellschaft Verfahrenstechnik und Chemieingenieurwesen (Hrsg.): VDI-Wärmeatlas.

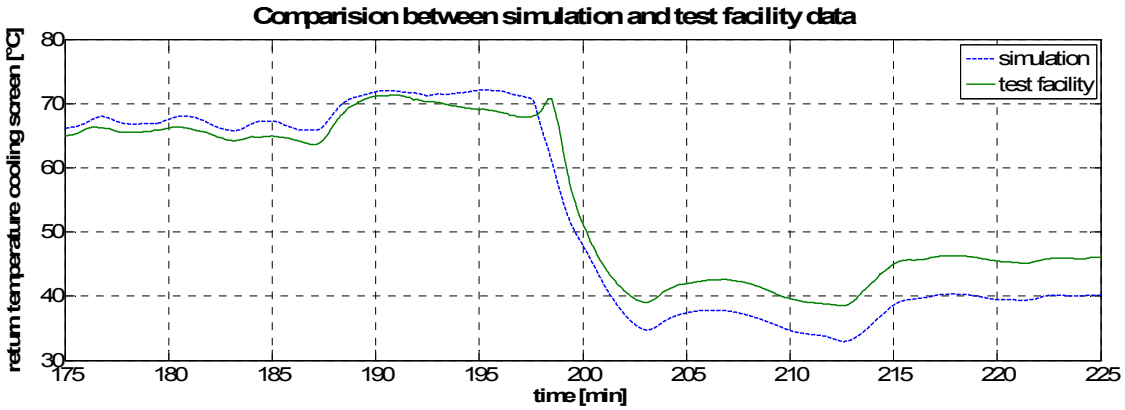

Figure 8: Comparison between simulation and test data for the return temperature of the cooling screen due to the break down of the coal mass flow

Zehnte, bearbeite und erweiterte Aufl. Berlin, Heidelberg: Springer, 2006

[7] Zbogar, A. et al.: Heat transfer in ash deposits: A modelling tool-box. In: Progress in Energy and Combustion Science 31 (2005), S. 371-421

[8] Kumar, V. et al.: Pressure drop and heat transfer study in tube-in-tube helical heat exchanger. In: Chemical Engineering Science 61 (2006), S. 4403-4416

[9] Vargas, S. et al.: Rheological properties of high-temperature melts of coal ashes and other silicates. In: Progress in Energy and Combustion Science 27 (2001), S. 237-429

[10] Hannemann, F. et al.: Application of Siemens Fuel Gasification Technology for different types of coal. 25th Annual Pittsburgh Coal Conference, Pittsburgh, PA, USA, September 29 – October 2, 2008

[11] Rezaei, H.R. et al.: Thermal conductivity of coal ash and slags and models used. In: Fuel 79 (2000), S. 1697-1710

[12] Seggiani, M: Modelling and simulation of time varying slag flow in a Prenflo entrained-flow gasifier. In: Fuel 77 (1998), Nr. 14, S. 1611-1621

